ChemComm

COMMUNICATION

View Article Online
View Journal | View Issue

Cite this: *Chem. Commun.*, 2015, 51, 6137

Received 28th November 2014,
Accepted 14th February 2015

DOI: 10.1039/c4cc09523e

www.rsc.org/chemcomm

Origin of SMM behaviour in an asymmetric Er(III) Schiff base complex: a combined experimental and theoretical study†

Chinmoy Das,‡ Apoorva Upadhyay,‡ Shefali Vaidya, Saurabh Kumar Singh, Gopalan Rajaraman* and Maheswaran Shanmugam*

An asymmetric erbium(III) Schiff base complex $[Er(HL)_2(NO_3)_3]$ was synthesized which shows SMM behaviour with an Ueff of 5.2 K. Dipolar interaction in 1 significantly reduced upon dilution which increases the barrier height to 51.5 K. *Ab initio* calculations were performed to shed light on the mechanism of magnetization relaxation.

An unprecedented effective energy barrier (U_{eff}) reported for a terbium phthalocyanin mononuclear single-molecule magnet (SMM) in 2003 was a milestone in molecular magnetism research compared to any transition metal clusters reported to date.[1] After this intriguing discovery, numerous monomeric and multinuclear lanthanide-based single-molecule magnet (SMM) flooded the literature.[2] In lanthanides, however, majority of the mononuclear SMM (more than 90%) reported are based on Dy(III) ion.[3] Moreover, several strategies have been proposed to increase the effective energy barrier of Dy(III)-containing SMMs.[4] Even after more than a decade of research effort, only four SMMs are known to date (in the absence of external bias field) with Er(III), and the all four are, however, organometallic mononuclear SMMs employing strong π electron donor ligands such as cyclooctatetraene (COT), cyclopentadienyl anion and its derivatives.[5] Among them, $[Er(COT)_2]$ complex holds the record blocking temperature of 12 K.[5d] Due to the scarcity of Er(III)-based SMMs in the literature, we chose to investigate the point charged ligand like Schiff base, namely 2-methoxy-6-[(*E*)-phenyliminomethyl]phenol (HL) rather than π-donor ligands, and its influence on the magnetization relaxation dynamics. In this communication, we report, for the first time in the literature, a highly unsymmetric Er(III) Schiff base complex which shows SMM behaviour in the absence of an external magnetic field, and its detailed electronic structure and plausible mechanism of relaxation is investigated in detail through computational studies.

One equivalent of lanthanum nitrate hydrate (Ln = Er^{3+} or Lu^{3+}) reacted with two equivalents of Schiff base ligand (HL) in ethanol; crystallization in methanol yielded orange coloured single crystals. Single crystal X-ray diffraction reveals the structure to be $[Ln(HL)_2(NO_3)_3]$ (where Ln = Er (**1**) (Fig. 1), Lu (**2**) (see Fig. S1 of ESI†)). Both **1** and **2** are structurally analogous; thus, we described the structure of **1** in detail. Both **1** and **2** crystallized in the orthorhombic space group, *Aba*2 (Table S1 of ESI†). The cationic charge of trivalent erbium ion is neutralized by three chelating nitrate ions, which accounts for six of the ten coordination sites. The remaining four coordination sites are occupied by the neutral HL ligand. However, the proton bound to phenolic oxygen in the free ligand migrates to the imine nitrogen atom (–C═N) and HL becomes zwitterionic (ZI) in nature before coordination to the Er^{III} ion. We have already proven the existence of the ZI nature of this Schiff base ligand[4b,6] and reports are known for other Schiff base containing lanthanide complexes.[7] Thus, the Er(III) ion exists with a ten-coordinate, distorted, bi-capped square anti-prismatic geometry determined by continuous shape measurement.[8]

The average bond distances of Er–O are found to be 2.4506 Å. Selected bond lengths and bond angles are given in Table S2 of the ESI.†

The detailed structural analysis of **1** reveals that the unit cell contains two molecules with the same molecular formula as mentioned above; however, the orientation of ligands are distinctly different from one another (a similar scenario was found in the unit cell of complex **2**). Between these two molecules, every ligating atom in one molecule is crystallographically distinct (**1a**, Fig. 1A), where the three nitrate ions are arranged in near trigonal planar arrangement with the two ZI Schiff base ligands arranged above and below the trigonal plane. Only half of the molecule is present in the unit cell for the second molecule (**1b**, Fig. 1B); the other half

Department of Chemistry, Indian Institute of Technology Bombay, Powai, Mumbai, Maharashtra, India-400076. E-mail: eswar@chem.iitb.ac.in, rajaraman@chem.iitb.ac.in; Fax: +91-22-2576-7192; Tel: +91-22-2576-7187

† Electronic supplementary information (ESI) available: Detailed synthesis and crystallographic information files are given along with necessary supporting dc and ac magnetic measurements. Computational details, computed energies of Kramers doublets and crystal field parameters of **1** and its model complexes along with the orientation of *g*-anisotropy for the respective species are given. CCDC 1036694 and 1047967. For ESI and crystallographic data in CIF or other electronic format see DOI: 10.1039/c4cc09523e

‡ Shares equal contribution.

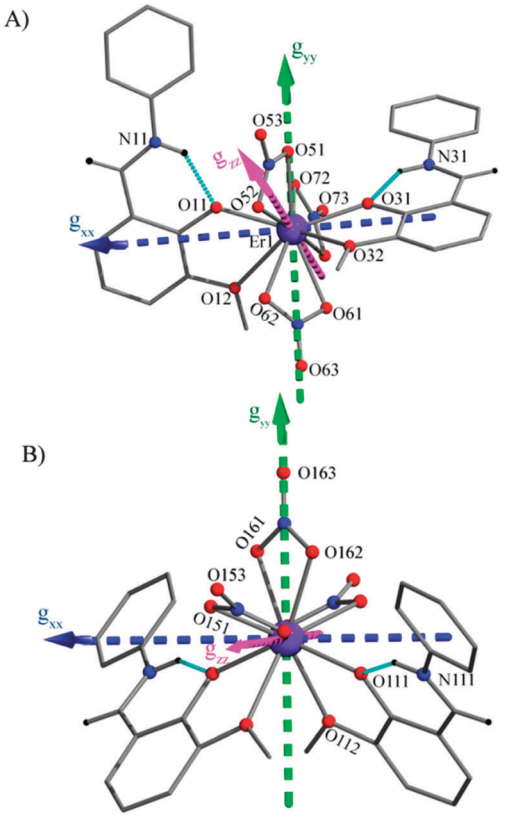

Fig. 1 Ball and stick representation of crystal structure of **1**. (A) Crystal structure of one of the molecules in the unit cell of **1**, where three nitrate ions are arranged in a nearly trigonal planar arrangement, (B) a geometric isomer (second molecule) with distinctly different orientation of nitrates and Schiff base ligands. The sky blue dotted bonds represent the intramolecular hydrogen bonding. The dotted arrows on both the molecules represent the *g*-anisotropy orientation. Colour code: purple = Er(III), blue = N, red = O, grey = C.

of the molecule is derived by inversion symmetry. In this molecule, the orientation of all the ligands (three nitrates and two ZI ligands) is different from that in **1a**. This is further confirmed by measuring the angles ∠NEr1N and ∠NEr2N (angles between nitrogen of nitrates and Er) to be 120° and 73.63° in **1a** and **1b**, respectively. The larger angle, ∠NEr1N, in **1a** compared to **1b** shows that the orientation of nitrates in both the molecules are different. The existence of such isomers within the same unit cell is very rare and has been reported by us recently, for the first time, in a Dy(III) analogue of complex **1**.[4b] The nitrates coordinated to **1a** and **1b** facilitate intermolecular hydrogen bonding and the atoms involved in such bonding are detailed in Table S3 of the ESI.†

Direct current (dc) magnetic susceptibility measurements were performed on a polycrystalline sample of **1** in the temperature range of 2.0–300 K with an applied magnetic field of 0.1 Tesla (Fig. 2). The room temperature (RT) $\chi_M T$ value of 11.48 cm^3 K mol^{-1} is observed for **1**, which is the expected value (11.47 cm^3 K mol^{-1}) with ground state term symbol of $^4I_{15/2}$ and g = 6/5. The $\chi_M T$ value decreases gradually from RT to 80 K, which could be possibly due to the depopulation of m_J levels. Below this temperature, the $\chi_M T$ value sharply decreased and reached 2.98 cm^3 K mol^{-1} at 2.0 K. Multiple factors could contribute to this drastic decrease in $\chi_M T$ value at low

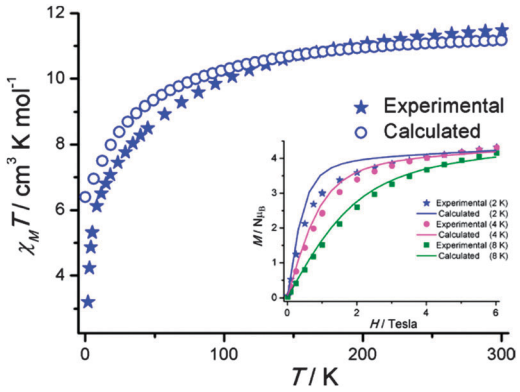

Fig. 2 Dc magnetic susceptibility measurement performed on a polycrystalline sample of **1** measured at 0.1 Tesla. The filled star represents the experimental data, the open circle represents the CASSCF + RASSI computed magnetic susceptibility from the crystal structure of **1**. Inset: field dependant magnetization measurement performed on the polycrystalline sample of **1** (symbols) at the indicated temperature. The solid lines represent the CASSCF + RASSI computed magnetization value of **1**.

temperatures such as magnetization blockage, intermolecular antiferromagnetic interaction and dipolar interaction.

Isothermal field dependent magnetization measurements performed on a polycrystalline sample of **1** show a sharp increase in magnetization at low field limit with a linear response to the magnetic moment upon increasing the magnetic field without any saturation (inset, Fig. 2). The considerably low magnetization value observed at high field limit (at 2.0 K) is indicative of magnetic anisotropy associated with complex **1**; such a scenario has been witnessed in many anisotropic metal complexes.[2a,9] The presence of magnetic anisotropy is further confirmed by the non-superimposable nature of the reduced magnetization curves (Fig. S2 of ESI†).

To investigate the magnetization relaxation dynamics, we performed ac susceptibility measurements with an ac amplitude of 1.0 Oe on a polycrystalline sample of **1** in the range of 0.5–8.0 K with and without an applied external magnetic field (Fig. 3A and Fig. S3 of ESI†). The ac data below 1.8 K were measured with the aid of IHelium3 setup. Complex **1** clearly shows a frequency dependent out-of-phase susceptibility (χ_M'') signal in the absence of an external dc magnetic field (Fig. 3A), which is a characteristic signature of a single-molecule magnet (SMM). Observation of this zero field SMM property for an asymmetric complex like **1** is quite rare, and it is

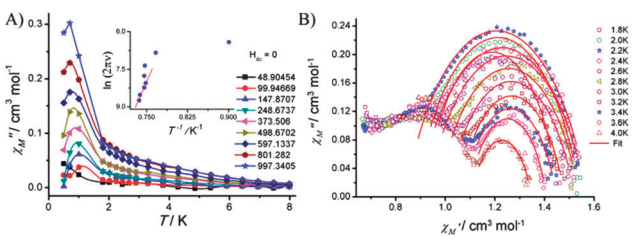

Fig. 3 (A) Alternating current magnetic susceptibility measurement performed on a polycrystalline sample of **1** (100%) showing the frequency dependent out-of-phase susceptibility signals (χ_M'') in the absence of an external magnetic field. Inset: Arrhenius plot constructed from ac relaxation dynamics of 50% diluted sample. (B) Cole–Cole plot derived from ac measurement of complex **1** (100%) in the presence of an optimum magnetic field of 0.5 Tesla.

the first example, to the best of our knowledge, to show zero field SMM behaviour with point charged ligands such as nitrates and HL ligand (see Table S4 in ESI†).[10]

To confirm the molecular origin of magnetization relaxation, ac susceptibility measurements were performed on 5% (data not shown) and 50% diluted sample of **1** (Fig. S4 of ESI†). The diluted samples were synthesized as per the synthetic method given in ESI† by taking the respective equivalence of $Ln(NO_3)_3{\cdot}xH_2O$ (where Ln = Er or Lu) according to the percentage dilution. From Fig. 3A, it is apparent that more than one relaxation processes are operating. The relaxation observed above 2.0 K is without a clear maxima; however, below 2.0 K, the maxima in χ_M'' is markedly visible in complex **1**. An Arrhenius plot was constructed from the ac measurements of 100% and 50% diluted sample of **1**, and the estimated anisotropic energy barrier (U_{eff}) for the magnetization relaxation was found to be 5.2 K (Fig. S5 of ESI†) and 51.4 K (inset of Fig. 3A) respectively. The increased U_{eff} of the 50% diluted sample of **1** unambiguously confirms that the relaxation dynamics are of molecular origin. Temperature-dependant heat capacity measurements performed on **1** undoubtedly show that there is no sign of a magnetic phase transition at low temperatures (Fig. S6 of ESI†). This further supports the fact that the observed χ_M'' signals are purely molecular in origin. The present study illustrates the importance of performing experiments at ultra-low temperatures because this offers, quantitatively, the barrier height for magnetization reversal. The observed energy barrier for **1**, however, is significantly lower than the organometallic Er(III) mononuclear SMM reported in the literature.[5a,c,d] Below 0.8 K (100%) and 1.3 K (50%), the Arrhenius plot deviates from linearity, which could be due to other faster relaxation processes such as QTM and/or direct processes and/or dipolar interactions in **1**. Such faster relaxation processes have been witnessed in other mononuclear SMMs reported in the literature.[2d,3,5a,11]

To suppress/quench the faster QTM relaxation processes in **1**, we performed ac measurements in the presence of an optimum dc bias field (0.5 Tesla). Frequency dependent χ_M'' signals were witnessed in a higher temperature (above 3.0 K) region; however, the signals were very broad without any maxima (see Fig. S3 of ESI†), which hindered the extraction of the magnetization reversal barrier. The Cole–Cole plot unambiguously confirms that more than one relaxation process is operational even in the presence of an external magnetic field (Fig. 3B). The major relaxation process was fitted to a generalised Debye model; α parameters varied from 0.16 to 0.29, suggesting that the moderate distribution of relaxation times could be due to weak dipolar interactions (Table S5 in the ESI†).

To analyse the *g*-tensors, relative energies of Kramers doublets (KDs), crystal field parameters, and to construct the *ab initio* blockade barrier, CASSCF + RASSI-SO calculations have been performed on complex **1** using MOLCAS 7.8 code.[12] Calculations were performed on both the geometrical isomers **1a** and **1b** with seven 4f orbitals and eleven 4f electrons in the active space (see ESI,† Tables S6–S10 in Computational details).

The computed energy window of all eight low-lying KDs for both structures **1a** and **1b** spanned over 494 and 499 cm^{-1}, respectively (see Tables S6 and S7, ESI†). The *g*-tensors in the ground state KD in **1a** (g_x = 1.03, g_y = 2.77, g_z = 13.99) and **1b** (g_x = 0.04, g_y = 0.07, g_z = 15.78) show axiality but lack pure Ising type

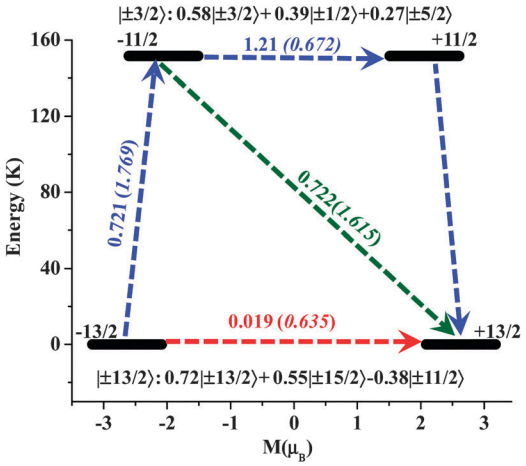

Fig. 4 Two low-lying Kramers doublets for **1b** along with possible relaxation pathways and the composition of wave functions of these KDs. The numbers provided are the computed transversal magnetic moments. Dashed blue and red lines show TA-QTM *via* first excited state and ground state QTM, respectively. Dashed green lines show the Orbach process. Numbers in parentheses are for molecule.

nature (g_{xx} = g_{yy} = 0, g_{zz} = 20) because both possess a significant transverse component. The computed orientation of principal magnetization axes (g_{zz}) are found to be oriented towards one of the O atoms (O(52)-Er-g_{zz} is titled by 11.8 degrees, see Fig. 1) of the attached $-NO_3$ ligand for both complexes **1a** and **1b** (see Fig. S7 and Tables S8 and S9, ESI†).

The wave function analysis shows a strong mixing of ground state with excited state m_J levels. Moreover, our calculations suggest that for both molecules **1a** and **1b**, a major contribution to the ground state comes from $|\pm13/2\rangle$ with significant mixing from other higher excited states as expected for a low-symmetric complex (Fig. 4). The principal magnetization axes of the first excited states are tilted by 86.8° and 90° from their ground states for **1a** and **1b**, respectively; this estimates the calculated barrier heights to be 70.4 K and 150.9 K, respectively (see Tables S8 and S9, Fig. S7, ESI† and Fig. 4). Although the computed spin Hamiltonian (SH) parameters reproduce the experimental magnetic data ($\chi_M T(T)$ and $M(H)$), some deviations at low temperatures (Fig. 2 and its inset) are observed. These deviations and the deviation observed between the computed magnetization barrier and the experimental effective energy barrier could be correlated to strong QTM predicted between the ground state KDs, hyperfine interactions and strong intermolecular interactions, which are likely to be present in complex **1** (closest metal–metal distance is 9.264(5) Å).[13] The existence of multiple relaxation processes even in the presence of a bias dc field (Fig. 3B) further strongly supports this observation. Dilution experiments ascertain this fact because the barrier height upon 50% dilution increases from 5.2 K to 51.4 K, suggesting that dipolar contributions are significant and even 50% dilution can enhance the barrier height by an order of magnitude.

Despite significant transverse anisotropy found for complex **1**, it exhibits zero field SMM behaviour, while the structurally analogous Dy(III) complex reported by us earlier exhibits field induced SMM behaviour.[4b] This suggests that the present ligand

environment better suits a prolate ion such as Er(III). Based on the electrostatic model recently proposed by Long and co-workers, the largest m_J value will be stabilized in a prolate Er(III) ion by engineering the ligand fields in equatorial positions around this ion.[14] This qualitative prediction is proven experimentally using COT and/or cp* ligands or in a three-coordinate Er(III) complex recently reported by Tang and co-workers.[5d,15] Undoubtedly, in complex **1**, in addition to the equatorial positions, point charged ligands are found in the axial position. The presence of four oxygen donor atoms (derived from two HL ligands) in axial positions in **1a** stabilizes $|\pm 13/2\rangle$ as the ground state. Besides, the low symmetry environment around Er(III) ion in **1a** leads to significant transverse anisotropy (Table S10 of ESI†). Even though molecule **1b** is also stabilized with an $|\pm 13/2\rangle$ ground state, the computed anisotropic energy barrier is larger than in **1a**. This is because **1b** contains only two oxygen donors (two phenoxo atoms of HL) in the axial position of the Er(III) ion. As the number of donor atoms decreases in the axial positions, the ground state-excited state gap increases. Furthermore, between the two geometrical isomers, **1b** is predicted to be more symmetric (lesser deviation (1.32) compared to ideal bi-capped square anti-prism geometry, as calculated by the SHAPE program[8]) than **1a** (deviation 1.83). This leads to more reduction in the transverse component in **1b** and diminishes the ground state QTM effect.

To probe this effect of ligand field on **1**, further calculations were performed on model complexes (see ESI,† Tables S11–S13 and Fig. S8 and S9). Two models have been constructed based on **1a** with the molecular formula of $[Er(HL)(NO_3)_3]$ (**1a**-A) and $[Er(NO_3)_3]$ (**1a**-B) by systematically removing the ZI Schiff base ligands, which were occupying the axial positions. The model complex **1a**-A with only one axial ligand field possesses a barrier height of 111.4 K with less transverse anisotropy as compared to complex **1a**. The model **1a**-B with no axial ligands stabilizes the m_J $|\pm 15/2\rangle$ as a ground state with a U_{eff} value of 189.1 K. The studies performed on model complexes evidently suggests that the presence of these axial ligands in complex **1** not only reduces the barrier height but also introduces significant transverse anisotropy leading to increase in QTM between the ground state KDs. This is also reflected in the computed crystal field parameters as well as the transversal magnetic moments (Fig. 4), which is consistent with a faster QTM between the ground state KDs for **1a** than **1b**.[16]

Apart from this relaxation process, thermally activated QTM (TA-QTM) and the Orbach process are also operational *via* the first excited state. Our calculations, for the first time, not only explain the observed differences between **1a** and **1b** but also suggest that an increase in axial ligands enhances the QTM in low-symmetry complexes like **1**.

In conclusion, the reported complex **1** serves as a surrogate marker to understand factors influencing the faster relaxation of magnetization and the role of the ligand field in determining the electronic structure of an Er(III) mononuclear SMM. The dilution experiment performed increased the barrier height by an order of magnitude. *Ab initio* calculations suggest that the presence of axial ligands not only diminishes the U_{eff} value but also introduces the transverse anisotropy at the ground state. We believe this study is the first of its kind to be undertaken in an asymmetric Er(III) complex and our conclusions are important for the design of novel Er(III)-based single-molecule magnets.

MS and GR acknowledge the Department of Science and Technology, DST (SR/S1/IC-32/2011) Nanomission (SR/NM/NS-1119/2011), IIT Bombay for financial support. GR thanks the Australian Research Council and the Australia-India AISRF for support. MS and GR thank Liviu Ungur and L. F. Chibotaru, Belgium for their additional MOLCAS routine.

Notes and references

1 N. Ishikawa, M. Sugita, T. Ishikawa, S.-Y. Koshihara and Y. Kaizu, *J. Am. Chem. Soc.*, 2003, **125**, 8694.
2 (*a*) H. L. C. Feltham and S. Brooker, *Coord. Chem. Rev.*, 2014, **276**, 1; (*b*) Y.-N. Guo, G.-F. Xu, Y. Guo and J. Tang, *Dalton Trans.*, 2011, **40**, 9953; (*c*) N. Ishikawa, *Polyhedron*, 2007, **26**, 2147; (*d*) R. A. Layfield, *Organometallics*, 2014, **33**, 1084; (*e*) R. Sessoli and A. K. Powell, *Coord. Chem. Rev.*, 2009, **253**, 2328; (*f*) D. N. Woodruff, R. E. P. Winpenny and R. A. Layfield, *Chem. Rev.*, 2013, **113**, 5110.
3 P. Zhang, Y.-N. Guo and J. Tang, *Coord. Chem. Rev.*, 2013, **257**, 1728.
4 (*a*) F. Habib, G. Brunet, V. Vieru, I. Korobkov, L. F. Chibotaru and M. Murugesu, *J. Am. Chem. Soc.*, 2013, **135**, 13242; (*b*) A. Upadhyay, K. Singh Saurabh, C. Das, R. Mondol, K. Langley Stuart, S. Murray Keith, G. Rajaraman and M. Shanmugam, *Chem. Commun.*, 2014, **50**, 8838; (*c*) K. Bernot, L. Bogani, A. Caneschi, D. Gatteschi and R. Sessoli, *J. Am. Chem. Soc.*, 2006, **128**, 7947; (*d*) I. Oyarzabal, J. Ruiz, J. M. Seco, M. Evangelisti, A. Camón, E. Ruiz, D. Aravena and E. Colacio, *Chem. – Eur. J.*, 2014, **20**, 14262.
5 (*a*) S.-D. Jiang, B.-W. Wang, H.-L. Sun, Z.-M. Wang and S. Gao, *J. Am. Chem. Soc.*, 2011, **133**, 4730; (*b*) J. J. Le Roy, I. Korobkov and M. Murugesu, *Chem. Commun.*, 2014, **50**, 1602; (*c*) J. J. Le Roy, L. Ungur, I. Korobkov, L. F. Chibotaru and M. Murugesu, *J. Am. Chem. Soc.*, 2014, **136**, 8003; (*d*) L. Ungur, J. J. Le Roy, I. Korobkov, M. Murugesu and L. F. Chibotaru, *Angew. Chem., Int. Ed.*, 2014, **53**, 4413; (*e*) K. R. Meihaus and J. R. Long, *J. Am. Chem. Soc.*, 2013, **135**, 17952.
6 (*a*) A. Upadhyay, C. Das, M. Shanmugam, S. K. Langley, K. S. Murray and M. Shanmugam, *Eur. J. Inorg. Chem.*, 2014, 4320; (*b*) A. Upadhyay, S. Vaidya, V. S. Venkatasai, P. Jayapal, A. K. Srivastava, M. Shanmugam and M. Shanmugam, *Polyhedron*, 2013, **66**, 87.
7 (*a*) J.-P. Costes, F. Dahan and F. Nicodeme, *Inorg. Chem.*, 2003, **42**, 6556; (*b*) W. Xie, M. J. Heeg and P. G. Wang, *Inorg. Chem.*, 1999, **38**, 2541.
8 (*a*) H. Zabrodsky, S. Peleg and D. Avnir, *J. Am. Chem. Soc.*, 1992, **114**, 7843; (*b*) H. Zabrodsky, S. Peleg and D. Avnir, *J. Am. Chem. Soc.*, 1993, **115**, 8278.
9 (*a*) N. Ahmed, C. Das, S. Vaidya, S. K. Langley, K. S. Murray and M. Shanmugam, *Chem. – Eur. J.*, 2014, **20**, 14235; (*b*) N. Ahmed, C. Das, S. Vaidya, A. K. Srivastava, S. K. Langley, K. S. Murray and M. Shanmugam, *Dalton Trans.*, 2014, **43**, 17375.
10 S. Demir, J. M. Zadrozny and J. R. Long, *Chem. – Eur. J.*, 2014, **20**, 9524.
11 (*a*) E. Lucaccini, L. Sorace, M. Perfetti, J.-P. Costes and R. Sessoli, *Chem. Commun.*, 2014, **50**, 1648; (*b*) M.-E. Boulon, G. Cucinotta, J. Luzon, C. Degl'Innocenti, M. Perfetti, K. Bernot, G. Calvez, A. Caneschi and R. Sessoli, *Angew. Chem., Int. Ed.*, 2013, **52**, 350.
12 F. Aquilante, L. De Vico, N. Ferre, G. Ghigo, P.-a. Malmqvist, P. Neograd y, T. B. Pedersen, M. Pitonak, M. Reiher, B. O. Roos, L. Serrano-Andres, M. Urban, V. Veryazov and R. Lindh, *J. Comput. Chem.*, 2010, **31**, 224.
13 F. Pointillart, K. Bernot, S. Golhen, B. Le Guennic, T. Guizouarn, L. Ouahab and O. Cador, *Angew. Chem., Int. Ed.*, 2015, **54**, 1504.
14 (*a*) J. D. Rinehart and J. R. Long, *Chem. Sci.*, 2011, **2**, 2078; (*b*) S. K. Singh, T. Gupta, M. Shanmugam and G. Rajaraman, *Chem. Commun.*, 2014, **50**, 15513; (*c*) S. K. Singh, T. Gupta and G. Rajaraman, *Inorg. Chem.*, 2014, **53**, 10835.
15 P. Zhang, L. Zhang, C. Wang, S. Xue, S.-Y. Lin and J. Tang, *J. Am. Chem. Soc.*, 2014, **136**, 4484.
16 L. Ungur, M. Thewissen, J.-P. Costes, W. Wernsdorfer and L. F. Chibotaru, *Inorg. Chem.*, 2013, **52**, 6328.

